# Stress effects on shallow-donor impurity states in symmetrical GaAs/$Al_xGa_{1-x}As$ double quantum wells

N. Raigoza,[1] A. L. Morales,[1] A. Montes,[1] N. Porras-Montenegro,[2] and C. A. Duque[1]
[1]*Instituto de Física, Universidad de Antioquia, AA 1226, Medellín, Colombia*
[2]*Departamento de Física, Universidad del Valle, AA 25360, Cali, Colombia*
(Received 17 April 2003; revised manuscript received 8 September 2003; published 30 January 2004)

The effects of the compressive stress on the binding energy and the density of shallow-donor impurity states in symmetrical GaAs/$Al_xGa_{1-x}As$ double quantum wells are calculated using a variational procedure within the effective-mass approximation. Results are for different well and barrier widths, shallow-donor impurity position, and compressive stress along the growth direction of the structure. We have found that independently of the well and barrier widths, for stress values up to 13.5 kbar (in the direct-gap regime) the binding energy increases linearly with the stress. For stress values greater than 13.5 kbar (indirect gap regime) and for impurities at the center of the wells, the binding energy increases up to a maximum and then decreases. For all impurity positions the binding energy shows a nonlinear behavior in the indirect gap regime due to the $\Gamma$-$X$ crossing effect. The density of impurity states is calculated for a homogeneous distribution of donor impurities within the barriers and the wells of the low-dimensional heterostructures. We have found that there are three special structures in the density of impurity states: one associated with on-center-barrier-, the second one associated with on-center-well-, and the third one corresponding to on-external-edge-well-impurity positions. The three structures in the density of impurity states must be observed in valence–to–donor-related absorption and conduction–to–donor-related photoluminescence spectra, and consequently these peaks can be tuned at specific energies and convert the system in a stress detector.

DOI: 10.1103/PhysRevB.69.045323 PACS number(s): 71.55.Eq; 78.67.De; 78.40.Fy

## I. INTRODUCTION

The development of molecular-beam epitaxy and metal-organic chemical-vapor deposition as a means of growing high-quality semiconductor heterostructures has led to the development of multilayered heterojunctions with atomically abrupt interfaces and precisely controlled compositional and doping profiles over distances as short as a few angstroms. If the layer thicknesses are sufficiently small, coupling between adjacent wells becomes important and causes superlattice formation. These superlattice structures have attracted considerable attention, both experimentally and theoretically, as they exhibit numerous interesting physical phenomena and have many device applications.[1–3] The latter include infrared detectors, resonant tunneling diodes, and ballistic transistors.

In isolated- and multiple-quantum-well systems consisting of alternate layers of GaAs and $Ga_{1-x}Al_xAs$, some authors have calculated the impurity binding energy with infinite or finite potential barrier height in the $Ga_{1-x}Al_xAs$ regions as functions of the GaAs well and $Ga_{1-x}Al_xAs$ barrier thickness and the position of the impurity which is located in the GaAs well.[4–7] For the isolated-quantum-well case, as a general feature, the authors present theoretical results for the optical-absorption and -photoluminescence spectra associated with a homogeneous distribution of donor and acceptor impurities along the quantum well structures, finding an edge associated with the maximum value of the impurity binding energy and one or two (depending on the external applied fields) van Hove–like singularities. Later on, with the purpose of achieving high electron mobility parallel to the GaAs well layers,[8] the modulated doping inside the $Ga_{1-x}Al_xAs$ has been considered.[9–11] In order to study exciton and shallow-donor states in symmetric-coupled GaAs-$Ga_{1-x}Al_xAs$ multiple quantum wells, the fractional-dimensional-space approach have been extended by Reyes-Gómez *et al.*[12] In this scheme, the real anisotropic ''exciton (or shallow donor) plus multiple-quantum-well'' semiconductor system was mapped, for each exciton (or donor) state, into an effective fractional-dimensional isotropic environment.

The problem of strain influence on optical properties of two-dimensional systems is very important from both fundamental and technical points of view. Previous theoretical and experimental investigations on the effect mostly considered direct optical transitions between valence- and conduction-band states. Kolokolov *et al.*[13] have found that the absorption of light with polarization parallel to the heterointerface in uniaxially stressed $p$-type GaAs/$Ga_{1-x}Al_xAs$ heteroestructures may be sensitive to the direction of light polarization. By photoluminescence studies on a GaAs-$Ga_{1-x}Al_xAs$ superlattice under hydrostatic pressure, Venkateswaran *et al.*[14] have reported the first observation of a transition involving a quantized energy level in the indirect $X$ conduction band, $E_{1h}^X$, and obtained its pressure coefficient. Using the effective-mass approximation, Gil *et al.*[15] have showed the importance of an accurate theoretical treatment of the Coulomb interaction, including intersubband mixings of valence wave functions, to describe subband-to-subband transition energies and oscillator strengths in asymmetrical GaAs-(Ga,Al)As double quantum wells (DQW's) under an uniaxial stress. Inter-Landau-level transitions have been reported by Smith *et al.*[1] in resonant tunneling between transverse $X$ states in GaAs/AlAs double-barrier structures under hydrostatic pressure. In this work they observed clear periodic

 ©2004 The American Physical Society

structures in the second derivative current-voltage characteristic of the resonance attributed to the processes $X_t(1) \rightarrow X_t(1) + \mathrm{TO}_{\mathrm{AlAs}}$, where $X_t(1)$ indicates the lowest quasiconfined subband associated with the transverse $X$ minima in AlAs and $\mathrm{TO}_{\mathrm{AlAs}}$ is a zone-center transverse optical phonon.

Theoretical works related to the effects of hydrostatic pressure and compressive stress on shallow-donor impurity states in GaAs-(Ga,Al)As quantum wells have been reported in the last ten years.[16–18] These authors have considered the $\Gamma$-$X$ crossover and, as general feature, they have found a linear dependence on the binding energy in the direct-gap regime under the applied pressure, while in the indirect-gap regime (applied pressure larger than 13.5 kbar) the energy grows with the pressure until reaching a maximum and then it decreases. Additionally, they have shown a redshift in the shallow-donor-related optical-absorption spectra associated with the pressure dependence of the semiconductor band gap.

It is well known that the application of uniaxial stress perpendicular to the growth axis of a QW provokes couplings between light- and heavy-hole states. This effect could produce interesting resonant-tunneling processes in multiple QW structures. Uniaxial stress and polarization-dependent measurements in GaAs/$\mathrm{Ga}_{1-x}\mathrm{Al}_x$As quantum wells under applied electric fields show that two peaks in the energy range where only a single exciton is expected to occur have strongly mixed heavy- and light-hole characters.[19] The pressure, magnetic field, and electric field effects on the excitonic systems in GaAs quantum wells have been reported by Bauer and Ando.[20] They have emphasized the phenomenon of exciton mixing induced by the complicated valence-band structure. Recently, Barticevic *et al.*[21] have reported the exciton trapping phenomena at interface defects/quantum dots in narrow QW's under an applied magnetic field. Results were obtained in the effective-mass approximation by an expansion of the exciton-envelope wave functions in terms of products of hole and electron QW states with appropriate Gaussian functions for the excitonic states.

The understanding of the optical properties associated with shallow-donor impurities in multiple GaAs-(Ga,Al)As quantum well structures is a subject of interest due to its potential application in optoelectronics, since it is possible to modulate the absorption spectra, by applying external pressures, from states of the valence band or the emission spectra from states of the conduction band, in both cases having as final states those related to randomly distributed donor impurities along the structure.

In the present work using the effective-mass approximation and the variational method, we make theoretical developments about the effects of an external compressive stress on the binding energy and the optical properties associated with shallow-donor impurities randomly distributed in symmetrical GaAs-(Ga,Al)As DQW structures. The image charge effects are not considered. The work is organized as follows: in Sec. II we present our theoretical framework, in Sec. III we give our results and discussion, and finally in Sec. IV we present our conclusions.

## II. THEORETICAL FRAMEWORK

In the effective-mass approximation, the Hamiltonian for a hydrogenic shallow-donor impurity in symmetrical GaAs-$\mathrm{Ga}_{1-x}\mathrm{Al}_x$As DQW under the effects of the temperature $(T)$ and of a compressive stress $(P)$ in the $z$ direction is given by

$$H = -\frac{\hbar^2}{2m^*_{w,b}(P,T)}\nabla^2 - \frac{e^2}{\varepsilon_{w,b}(P,T)r} + V(z,P,T), \quad (1)$$

where $r=[x^2+y^2+(z-z_i)^2]^{1/2}$ is the carrier-impurity distance and subscripts $w$ and $b$ stand for the quantum well (WL) and the barrier layer (BL) materials, respectively. $m^*_{w,b}(P,T)$ are the WL and BL material parabolic conduction effective masses as functions of $P$ and $T$ (Ref. 22):

$$m_w(P,T) = \left[1 + 7.51\left(\frac{2}{E_g(P,T)} + \frac{1}{E_g(P,T)+0.341}\right)\right]^{-1} m_0, \quad (2)$$

where $E_g(P,T)$ eV is the stress-dependent band gap for the GaAs semiconductor at the $\Gamma$ point and at low temperatures, which is expressed as[23]

$$E_g(P,T) = 1.519 + 10.7\times 10^{-3}P - 5.405 \times 10^{-4}T^2/(T+204). \quad (3)$$

The barrier effective mass depends on the aluminum concentration $(x)$ as

$$m_b = m_w + 0.083 x m_0. \quad (4)$$

We stress that for single QW's larger than 50 Å, the nonparabolic effective-mass effects are lower than 5%.[24] $\varepsilon_{w,b}(P,T)$ are the WL and BL material static dielectric constants. At $T=4$ K the stress-dependent GaAs static dielectric constant is given by[25]

$$\varepsilon_w(P,4K) = 12.83\exp(-1.67\times 10^{-3}P). \quad (5)$$

The dielectric constant mismatch effects in single GaAl-(Ga,Al)As quantum wells have been reported showing that the main effects are for small well widths and high Al concentration.[26] For example, for $x=0.3$ and $L=100$ Å the difference is the order of 2% diminishing with increasing well size. Strictly speaking, the image potential in QW's cannot be neglected in considering electronic and impurity states, especially when the dimensions of the wells are small[27] (well sizes of 50 Å imply a 9% difference in binding energy).

In our calculations we use $x=0.3$ and the structures are generally with large sizes. Due to the fact that in the present work we focus our attention on stress effects, charge image effects have not been considered. This means that in the Hamiltonian in Eq. (1) $\varepsilon_b(P,T)=\varepsilon_w(P,T)$.[28]

$V(z,P,T)$ is the potential which confines the donor electron in the WL regions, given by

$$V(z,P,T)=\begin{cases} V_0(P,T), & \text{for } |z|>L_c \text{ and } |z|<L_b/2, \\ 0, & \text{for } L_b/2<|z|<L_c, \end{cases} \tag{6}$$

where $L_c=L_b/2+L_w$ with $L_b$ and $L_w$ the stress-dependent width of the central BL and the width of a single WL, respectively. $V_0(P,T)$ is the stress-dependent barrier height.[16] $L_b$ and $L_w$ can be obtained by the fractional change in volume, which for the zinc-blende crystal of volume $V$ is given by[29]

$$\frac{\delta V}{V}=-3P(S_{11}+2S_{12}), \tag{7}$$

where $S_{11}$ $(=1.16\times10^{-3}\ \text{kbar}^{-1})$ and $S_{12}$ $(=-3.7\times10^{-4}\ \text{kbar}^{-1})$ are the elastic constants of GaAs.[16]

Following Chen and Zhou,[10] the trial wave function for the ground state is chosen as

$$\Psi(r)=Nf(z)g(r), \tag{8}$$

where $N$ is a normalization constant,

$$g(r)=\exp(-\lambda r) \tag{9}$$

is the hydrogenic part, and $f(z)$ is the eigenfunction of the Hamiltonian in Eq. (1) without the impurity potential term, which is given by

$$f(z)=\begin{cases} +A\exp[\beta(z+L_c)], & z\leqslant -L_c, \\ -B\sin\left[\eta\left(z+\frac{L_b}{2}\right)\right]+C\cos\left[\eta\left(z+\frac{L_b}{2}\right)\right], & -L_c<z<-\frac{L_b}{2}, \\ +\cosh(\beta z), & -\frac{L_b}{2}<z<\frac{L_b}{2}, \\ +B\sin\left[\eta\left(z-\frac{L_b}{2}\right)\right]+C\cos\left[\eta\left(z-\frac{L_b}{2}\right)\right], & +\frac{L_b}{2}<z<+L_c, \\ +A\exp[-\beta(z-L_c)], & z\geqslant +L_c \end{cases} \tag{10}$$

The coefficients $A$, $B$, and $C$ are obtained from the matching conditions of the eigenfunction $f(z)$ at the interfaces.

The corresponding eigenvalue associated with $f(z)$, $E_0(P)$, may be obtained as the first root of the transcendental equation

$$2\cos(\eta L_w)+\left(\mu-\frac{1}{\mu}\right)\sin(\eta L_w)-\left(\mu+\frac{1}{\mu}\right)\sin(\eta L_w)\times\exp(-\beta L_b)=0, \tag{11}$$

where $\mu=m_w^*\beta/m_b^*\eta$ and $\eta$ and $\beta$ are, respectively,

$$\eta=\left[\frac{2m_w^*(P)}{\hbar^2}E_0(P)\right]^{1/2} \tag{12}$$

and

$$\beta=\left\{\frac{2m_b^*(P)}{\hbar^2}[V_0(P)-E_0(P)]\right\}^{1/2}. \tag{13}$$

The compressive stress dependence of the donor binding energy is calculated from the definition

$$E_b(P)=E_0(P)-E_{\min}(P), \tag{14}$$

where $E_{\min}(P)$ is the eigenvalue with the impurity potential term, minimized with respect to the variational parameter $\lambda$.

In the next section, our results for a symmetrical GaAs-$Ga_{0.7}Al_{0.3}As$ DQW are presented at $T=4$ K.

## III. RESULTS AND DISCUSSION

In Fig. 1 we can observe the symmetry of the probability density with the impurity located at the center of the barrier (solid lines), as well as its asymmetry when the impurity is located at the center of the right well of the symmetrical GaAs-(Ga,Al)As DQW for two values of the applied stress, 10 kbar [Fig. 1(a)] and 30 kbar [Fig. 1(b)]. An absolute maximum in the probability density at the center barrier impurity position, $P=30$ kbar, is observed, in contrast for the case for $P=10$ kbar where the maximum occur at the wells. This difference is due to the increasing stress which in the limit of 37 kbar makes the barrier equal to zero and the probability density becomes the same as a hydrogenic atom [see the inset in Fig. 1(b)]. The dashed lines show the probability density for impurities at the center of the right well where, independently of the applied stress, the absolute maximum is located at the impurity position, according to the 37 kbar limit. Due to the larger coupling of the wells for the $P=30$ kbar case, the probability density to the left well is larger than the one in Fig. 1(a)—e.g., for $L_b=50$ Å—and for 10, 30, and 35 kbar applied stresses the percentage of probability density in the barrier and the left well is 30%, 37%, and 43%, respectively.

Figure 2 shows the binding energy of a donor impurity as a function of the growth direction impurity position in two symmetrical GaAs-(Ga,Al)As DQW's and different values of the applied compressive stress. In all curves it is observed how the binding energy increases as the impurity position goes from the center of the barrier to reach a maximum when

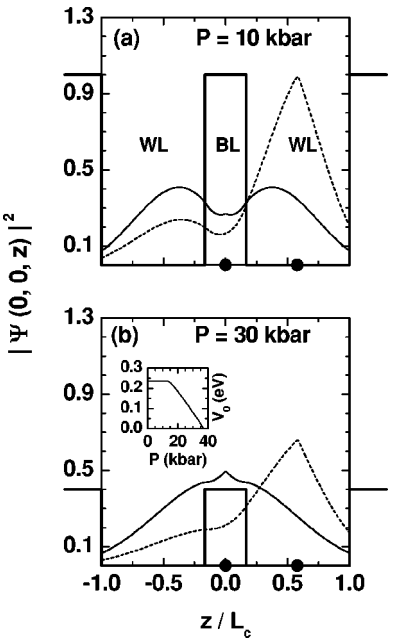


FIG. 1. $z$-direction probability density of a donor impurity in symmetrical GaAs-(Ga,Al)As DQW's with $L_w = 50$ Å and $L_b = 20$ Å, for $P = 10$ kbar (a) and $P = 30$ kbar (b). The solid and dashed lines are for barrier-center and right well-center impurity positions (solid circles). The inset in (b) shows the stress dependence of the barrier height.

the impurity is in the well region and then diminishes when the impurity is close to the well edge. For an impurity located at the center of the barrier the binding energy increases with the decrease of the barrier width for a given value of the stress. However, as observed, at the well region there is a crossing between the corresponding solid and dashed curves, at constant applied stress, because the binding energy increases faster with increasing barrier width, which is equivalent to a higher confinement.

It is important to note that for an applied stress in the direct-gap regime smaller than 13.5 kbar, the binding energy curves always move to higher energy with the increment of the stress, independent of the impurity position (there are no

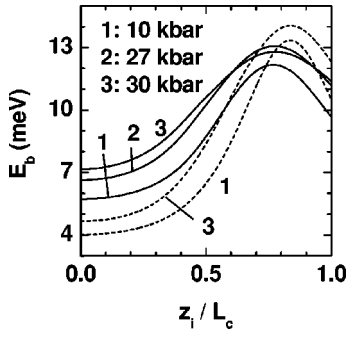


FIG. 2. Binding energy of a donor impurity as a function of the growth direction impurity position in symmetrical GaAs-(Ga,Al)As DQW's. The sizes of the two considered structures are $L_w = 50$ Å, $L_b = 100$ Å (solid lines) and $L_w = 50$ Å, $L_b = 200$ Å (dashed lines). Different values of the applied compressive stress are considered.

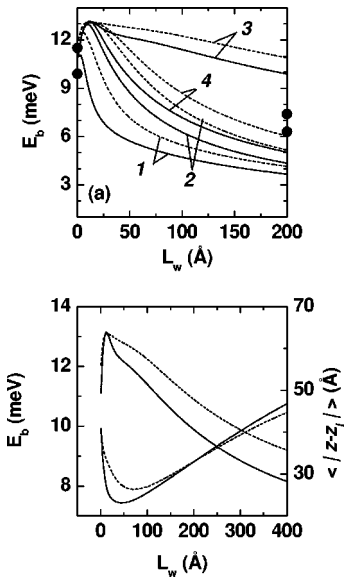


FIG. 3. (a) Binding energy of a donor impurity as a function of the width of the wells in symmetrical GaAs-(Ga,Al)As DQW's with $L_b = 200$ Å for $P = 10$ kbar (solid lines) and $P = 30$ kbar (dashed lines). Numbers 1, 2, 3, and 4 are for the impurity located at the barrier center, at the barrier edge, at the well center, and at the well edge, respectively. (b) The binding energy for well center impurities [curves 3 in (a)] showing a slow change, at low values of well width, due to the coupling of the wells. The lower curves for the expectation value of $|z-z_i|$ show the origin of the binding energy behavior (see text for discussion).

crossings) (this is not shown in the figure). For stress in the indirect-gap regime the same behavior continues for impurities close to the center of the barrier. However, for impurities close to the center of the well it is observed that, in the indirect-gap regime, the binding energy grows with the stress, until reaching a maximum value, and then it falls down (see Fig. 5). This behavior is associated with the crossings of solid curves marked with 2 and 3 at the impurity positions given by 0.6 Lc and 0.9 Lc. Whenever these crossings are present, the curves of binding energy as a function of applied stress, for that value of the impurity position (where the crossing is given), present a maximum. These crossings are interesting since two structures of different dimensions can be tuned to the same energy using two different values of the impurity position (solid curve 1 and dashed curve 1), or one structure with two different impurity positions can be tuned with two different stresses (solid curves 2 and 3).

The role of the quantum confinement is displayed in Fig. 3(a), where the binding energy for different impurity positions as a function of the well width (the widths of the wells increase simultaneously) in symmetrical GaAs-(Ga,Al)As DQW's is shown. As a general feature, we observe that the binding energy increases for small well sizes, until reaching a maximum value, and then diminishes with increasing well width as expected due to the weakness of the geometric confinement. At the maximum binding energy the distance between the impurity and electron cloud reaches its minimum value. The important feature in this figure is that curve 3

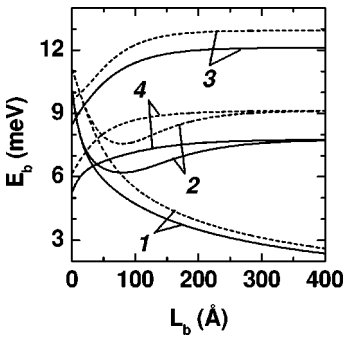


FIG. 4. Binding energy of a donor impurity as a function of the barrier width in symmetrical GaAs-(Ga,Al)As DQW's with $L_w = 100$ Å for $P = 10$ kbar (solid line) and $P = 30$ kbar (dashed line). Numbers 1, 2, 3, and 4 are the same as those in Fig. 3.

shows a flatter binding energy behavior as compare to the other ones. This can be understood by noting that in positions 1, 2, and 4 the electron cloud has more space to distribute itself (see Fig. 1 for the impurity position at the well and barrier center) while for position 3, with a large barrier width of 200 Å, the electron cloud is confined to just one well space and has less freedom to move, so the distance to the impurity remains almost constant. It is interesting to remark that in the zero-well-width limit—that is, for bulk $Ga_{0.7}Al_{0.3}As$—the binding energy does recover the value of 1 effective rydberg for the two values of the stress (see the two solid circles at the left axis). For large values of the well width, it is relevant to note that the binding energy for impurities located at the well center goes to the exact limit of a hydrogenic atom in GaAs for the two values of the stress (see the two solid circles at the right axis for 1 effective rydberg corresponding to 10 and 30 kbar). In Fig. 3(b), it is worth noting the change in the form of the binding energy for curves 3, due to the large confinement of the electron cloud at small values of $L_w$. For the case of large applied stress, dashed curve 3, the decrease in barrier width produces a smaller confinement. The variation of the $|z - z_i|$ expectation value confirms the above discussion. In spite of the fact that we neglected image charge effects we should notice that there will be important changes in Fig. 3 for well widths lower than 50 Å when these effects are included.

The effects of the central barrier width on the binding energy for different impurity positions and two values of the applied compressive stress are shown in Fig. 4. When the barrier width goes to the zero, we reproduce the exact values for the binding energy in a single quantum well of 200 Å.[30] It is clear that in this zero-$L_b$ limit curves 1 and 2 with solid lines (dashed lines) should go to the same binding energy value. On the other hand, in the limit of large barrier width the results converge to the binding energy values for 100 Å decoupled quantum wells.[30] Additionally, in the $L_b$ infinite limit, for an applied stress smaller than 37 kbar, when the impurity is located at the center of the barrier [see also Fig. 1(a)] the binding energy will always go to zero because the expectation value of the electron-impurity distance is going to infinity and therefore the Coulomb interaction goes to zero. It is clear that for on-center and on-edge well impurities, the wells coupling become evident for $L_b$ less than 200 Å.

The characteristic behavior of curves 2, 3, and 4 can be analyzed in the following way.

For curves 4: initially, $L_b = 0$, the wave function is allowed to extend in the well region for 200 Å. As the barrier growths this region begins to be restricted to 100 Å, but for relatively small barriers the region extends a little toward the left well: for that reason the binding energy increases until the barrier becomes sufficiently large as to impede the wave function penetration toward the second well, and as a consequence a constant-energy-limit situation is reached. A similar behavior is found for position 3 (on-center well impurity): in this case the wave function can extend to 50 Å in the well region to the right and 150 Å toward the left, as the barrier width increases the allowed left region begins to be restricted to 50 Å since the barrier begins to uncouple the left well. For impurities at the border of the barrier (curves 2) the behavior is very different. Initially the wave function is totally symmetrical with respect to the impurity position, and since the well is of 200 Å, the effect of the external barriers is very low: as a consequence the binding energy is very high. When the barrier appears it breaks the wave function spatial symmetry, increasing the carrier-impurity distance expectation value and therefore the binding energy decreases as a result of the decreasing Coulomb interaction. However, for $L_b < 100$ Å the effect of the well to the left is manifested in an allowed region of the order of 100 Å to the left of the impurity and another of 100 Å to the right. When $L_b$ increases, the well to the left is uncoupled and the wave function will be confined in a region of 100 Å that corresponds to the well at the right. This manifests itself in a binding energy increase because the carrier-impurity distance expectation value is restricted to approximately 100 Å—i.e., an increment in Coulomb interaction. The binding energy grows toward the limit in which the left well disappears, and due to this fact, it will join with the corresponding value for the impurity located at the external side of the well (which corresponds the merging of curves 2 and 4).

The compressive stress dependence of the binding energy for different impurity positions in symmetrical GaAs-(Ga,Al)As DQW's for two different values of the well and barrier widths is presented in Fig. 5. As observed, for stress values up to 13.5 kbar (vertical solid line) the binding energy increases linearly with the stress. This is due to the increment of the barrier and well effective masses as well as to the decrement of the dielectric constant with stress. For stress values higher than 13.5 kbar it is well known that the $\Gamma$-$X$ crossover shows up in GaAs, diminishing the barrier height with stress, causing the variation observed in the binding energy (see the inset in Fig. 1).[17,18,30] It is important to remark that for stress values around 37 kbar there is a semiconductor-metal transition.

For curves 1, corresponding to an on-center barrier impurity, as the stress increases the barrier height diminishes and the wave function penetrates into the central barrier and therefore a decrease in the carrier-impurity distance expectation value is found, giving an increment of the binding energy. For small barrier widths, the binding energy shows a

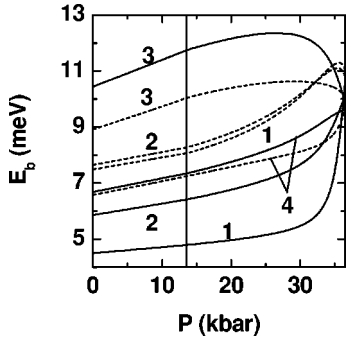


FIG. 5. Binding energy of a donor impurity as a function of the applied compressive stress in symmetrical GaAs-(Ga,Al)As DQW's with $L_w = L_b = 100$ Å (solid line) and $L_w = 75$ Å and $L_b = 25$ Å (dashed line). Numbers 1, 2, 3, and 4 are the same than those from Fig. 3.

softer variation since, for low stress, the charge distribution is more concentrated around the impurity. A similar situation happens for impurities at the two walls of the well.

For the well dimensions here considered, for on-center well impurities the variation observed in the binding energy with stress presents a very similar behavior to the one observed for impurities at the center of isolated single quantum wells.[30]

The binding energy of a donor impurity as a function of the impurity position along the growth direction in symmetrical GaAs-(Ga,AlAs) DQW's and the corresponding density of impurity states (DOIS) is presented in Fig. 6. We observe two structures in the DOIS associated with the minimum of the binding energy at the on-center barrier and to the maximum of the binding energy at the well region. From these results we can infer a direct correspondence between the impurity position-dependent binding energy and the DOIS. As observed in the binding energy as a function of the impurity position, for each applied stress, there is a double contribution to the DOIS for energies higher than the value corresponding to the binding energy of the impurity located at the center of the barrier. For example, this fact is associated with the drastic change of the DOIS close to 7.3 meV

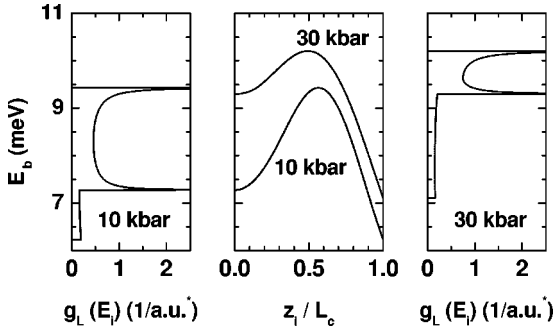


FIG. 6. Binding energy of a donor impurity as function of the growth direction impurity position in symmetrical GaAs-(Ga,Al)As DQW's with and $L_w = 100$ Å and $L_b = 20$ Å and for an applied compressive stress of 10 kbar (lower curve) and 30 kbar (upper curve). The plots to the right ($P = 30$ kbar) and the left ($P = 10$ kbar) correspond to the density of impurity states.

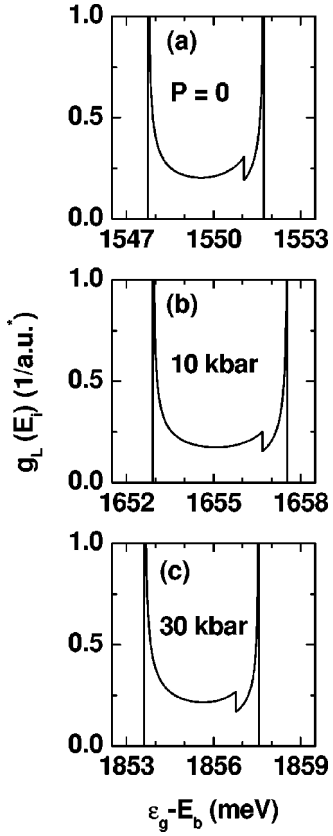


FIG. 7. Density of impurity states as a function of the difference between the effective energy gap (energy of the first state for electrons + energy of the first state for holes + energy of the GaAs band gap) and the impurity $z$-position-dependent binding energy in symmetrical GaAs-(Ga,Al)As DQW's. The dimensions of the structure are $L_w = 100$ Å and $L_b = 50$ Å, and different values of the applied compressive stress have been used.

for $P = 10$ kbar. Additionally, for the same case it can be observed the quasiconstant value of the DOIS for binding energies between 6.2 and 7.3 meV. This is a signature of the quasilinear behavior of the binding energy of impurities located close to the external on-edge of the quantum wells. This quasiconstant DOIS feature is a consequence of the well coupling occurring for small values of $L_b$.

In Fig. 7 we display the donor DOIS as a function of the difference between the effective energy gap [$\varepsilon_g$ = energy of the first state for electrons + energy of the first state for holes + energy of the GaAs band gap] and the impurity binding energy for different values of the applied compressive stress. Notice that for the different values of the applied stress, the drastic change in the DOIS is localized between the two structures of infinite weight, different from the results in Fig. 6 due to the larger value of $L_b$. When the stress approximates to the limit value of 37 kbar [see the inset in Fig. 1(b)], the DOIS must approximate to only one structure at energy of 1 effective rydberg for the GaAs. This fact begins to be evident in the approaching of the two sharp structures [Fig. 7(c)] when the stress increases. Otherwise, in curves for 0 and 10 kbar [Figs. 7(a) and 7(b), respectively] a separation between the two structures due to the linear be-

havior of the effective mass and the dielectric constant with the applied stress is observed. The shift to higher energies of the DOIS is due basically to the stress dependence of the GaAs-(Ga,Al)As band gap and this must conduce to a *red-shift* of the donor-related absorption spectra with the compressive stress.[17]

## IV. CONCLUSIONS

The effects of the compressive stress on the binding energy and the shallow-donor DOIS in symmetrical $GaAs/Al_xGa_{1-x}As$ DQW are calculated using a variational procedure within the effective-mass approximation. Results are for different well and barrier widths, shallow-donor impurity position, and compressive stress along the growth direction of the structure.

For an impurity located at the center of the barrier the binding energy increases with the decrease of $L_b$ for a given value of the applied stress (Fig. 2). However, in the well region there is a crossing for different values of the barrier width because the binding energy increases faster with increasing barrier width, which is equivalent to a higher confinement.

The impurity confinement due to the decrease in the well width [Fig. 3(a)] produces an increase in the binding energy up to a maximum value. A characteristic structure is found in the binding energy [Fig. 3(b)] when the barrier height decreases due to the coupling of the wells, as a result of the wave function penetration into the central barrier.

The effects of the barrier width on the binding energy for different impurity positions and two values of the applied compressive stress are shown in Fig. 4. When the barrier width goes to the zero, we reproduce the exact values for the binding energy in a single quantum well with well width of 200 Å.[30] On the other hand, when the barrier width increases the results converge to the values of the binding energy for 100 Å decoupled quantum wells and for different impurity positions.[30]

For barrier widths less than 200 Å the binding energy behavior is detected by the coupling of the two wells and by the impurity position. For larger barrier widths the wells are uncoupled, giving a constant-binding-energy behavior, except for the on-center barrier impurity position in which the binding energy goes to zero.

We have found that independently of the well and barrier dimensions, for stress values up to 13.5 kbar the binding energy increases linearly with stress. For stress values larger than 13.5 kbar and for impurities at the center of the wells, the binding energy increases up to a peak and then decreases. This behavior produces a crossing of the binding energy curves as a function of the impurity position for equal dimensions but stresses of 27 kbar and 30 kbar. For impurities close to the barrier center and close to the well edges, the binding energy, as a function of the stress (Fig. 5), shows a nonlinear behavior in the indirect-gap regime.

The DOIS (Figs. 6 and 7) is a direct consequence of the binding energy variation with impurity position. The DOIS is calculated for a homogeneous distribution of donor impurities within the barriers and the wells of the symmetrical GaAs-(Ga,Al)As DQW. We have shown that there are three special structures in the DOIS: one associated with on-center-barrier-, the second one associated with on-center-well-, and the third one corresponding to on-external-edge-well-impurity positions. The three structures in the DOIS must be observed in valence–to–donor-related absorption and conduction–to–donor-related photoluminescence spectra, and consequently these peaks can be tuned at specific energies and convert the system into a stress detector. Also, we have observed that the DOIS depends strongly on the applied stress. Theoretical calculations on shallow-donor-related absorption and photoluminescence spectra in asymmetrical GaAs-(Ga,Al)As DQW's under compressive and extensive stress will be published elsewhere.

By considering the heavy- and light-hole valence-band mixing, the present work could be extended to consider the stress effects on the binding energy and optical properties associated with shallow-acceptor impurities and excitonic complexes. This work is in process and will be published elsewhere.

## ACKNOWLEDGMENTS

The authors are grateful to the Universidad de Antioquia (CODI) for financial support. This work was financed in part by Colciencias, the Colombian Scientific Agencies, under Grant Nos. 1115-05-11502 and 1106-05-11498.

[1] J. M. Smith, P. C. Klipstein, R. Grey, and G. Hill, Phys. Rev. B **57**, 1740 (1998).

[2] N. Dai, D. Huang, X. Q. Liu, Y. M. Mu, W. Lu, and S. C. Shen, Phys. Rev. B **57**, 6566 (1998).

[3] K. I. Kolokolov, A. M. Savin, S. D. Beneslavski, N. Ya. Minina, and O. P. Hansen, High Press. Res. **18**, 69 (2000).

[4] G. Bastard, Phys. Rev. B **24**, 4714 (1981).

[5] C. Mailhiot, Y. C. Chang, and T. C. McGill, Phys. Rev. B **26**, 4449 (1982).

[6] L. E. Oliveira and R. Pérez-Alvarez, Phys. Rev. B **40**, 10 460 (1989); L. E. Oliveira and J. López-Gondar, *ibid.* **41**, 3719 (1990); R. B. Santiago, L. E. Oliveira, and J. d'Albuquerque e Castro, *ibid.* **46**, 4041 (1992).

[7] A. Latgé, N. Porras-Montenegro, M. de Dios-Leyva, and L. E. Oliveira, J. Appl. Phys. **81**, 6234 (1997).

[8] R. Dingle, H. Stormer, A. C. Gossard, and W. Wiegmann, Appl. Phys. Lett. **23**, 665 (1978).

[9] S. Chaudhuri, Phys. Rev. B **28**, 4480 (1983).

[10] H. Chen and S. Zhou, Phys. Rev. B **36**, 9581 (1987).

[11] N. Nguyen, R. Ranganathan, B. D. McCombe, and M. L. Rustgi, Phys. Rev. B **44**, 3344 (1991); **45**, 11 166 (1992).

[12] E. Reyes-Gómez, A. Matos-Abiague, C. A. Perdomo-Leiva,

M. de Dios-Leyva, and L. E. Oliveira, Phys. Rev. B **61**, 13 104 (2000).
[13] K. I. Kolokolov, S. D. Beneslavski, N. Ya. Minina, and A. M. Savin, Phys. Rev. B **63**, 195308 (2001).
[14] U. Venkateswaran, M. Chandrasekhar, H. R. Chandrasekhar, T. Wolfram, R. Fischer, W. T. Masselink, and H. Morkoç, Phys. Rev. B **31**, 4106 (1985).
[15] B. Gil, P. Lefebvre, P. Bonnel, H. Mathieu, C. Deparis, J. Massies, G. Neu, and Y. Chen, Phys. Rev. B **47**, 1954 (1993).
[16] See A. M. Elabsy, J. Phys.: Condens. Matter **6**, 10 025 (1994), and references therein.
[17] S. Y. López, N. Porras-Montenegro, and C. A. Duque, Phys. Status Solidi C **0**, 648 (2003).
[18] A. L. Morales, A. Montes, S. Y. López, N. Raigoza, and C. A. Duque, Phys. Status Solidi C **0**, 652 (2003).
[19] R. T. Collins, L. Viña, W. I. Wang, L. L. Chang, L. Esaki, K. v. Klitzing, and K. Ploog, Phys. Rev. B **36**, 1531 (1987).
[20] G. E. W. Bauer and T. Ando, Phys. Rev. B **38**, 6015 (1988).
[21] Z. Barticevic, M. Pacheco, C. A. Duque, and L. E. Oliveira, Phys. Rev. B **68**, 073312 (2003).
[22] S. Adachi, J. Appl. Phys. **58**, R1 (1985).
[23] A. M. Elabsy, J. Phys.: Condens. Matter **6**, 10 025 (1994).
[24] S. Chaudhuri and K. K. Bajaj, Phys. Rev. B **29**, 1803 (1984); K. Jayakumar, S. Balasubramanian, and M. Tomak, *ibid.* **33**, 4002 (1986); W. Chen and T. G. Andersson, *ibid.* **44**, 9068 (1991).
[25] G. A. Samara, Phys. Rev. B **27**, 3494 (1983).
[26] A. M. Elabsy, Phys. Rev. B **46**, 2621 (1992); Z. Y. Deng, T. R. Lai, and J. K. Guo, *ibid.* **50**, 5732 (1994).
[27] Z. Y. Deng, T. R. Lai, J. K. Guo, and S. W. Gu, J. Appl. Phys. **75**, 7389 (1994).
[28] C. A. Duque, A. L. Morales, A. Montes, and N. Porras-Montenegro, Phys. Rev. B **55**, 10 721 (1997); A. Latgé, N. Porras-Montenegro, M. de Dios-Leyva, and L. E. Oliveira, *ibid.* **53**, 10 160 (1996); A. Bruno-Alfonso, M. de Dios-Leyva, and L. E. Oliveira, *ibid.* **57**, 6573 (1998).
[29] P. Y. Yu and M. Cardona, *Fundamentals of Semiconductors* (Springer-Verlag, Berlin, 1998).
[30] A. L. Morales, A. Montes, S. Y. López, and C. A. Duque, J. Phys.: Condens. Matter **14**, 987 (2002).